Diagn Interv Radiol 2011; 17:3–9

NEURORADIOLOGY
ORIGINAL ARTICLE

Evaluation of jugular foramen nerves by using b-FFE, T2-weighted DRIVE, T2-weighted FSE and post-contrast T1-weighted MRI sequences

Hasan Aydın, Elif Altın, Alper Dilli, Serdar Sipahioğlu, Baki Hekimoğlu

PURPOSE
To assess the most effective magnetic resonance imaging (MRI) sequence for the visualization of the 9th, 10th, and 11th cranial nerves (glossopharyngeal, vagus, and accessory nerves, respectively) in their intraforaminal/canalicular courses.

MATERIALS AND METHODS
Balanced fast-field echo (b-FFE), 3D-T2W DRIVE, T2W 2D TSE and post-contrast T1W MRI sequences were all applied and we tried to get the best sequence for the exact assessment of the 9th, 10th, and 11th cranial nerves. Six hundred nerves of 100 patients without symptoms of neurovascular compression were examined using the above sequences. Imaging analysis was graded as: a) nerves analyzed by certainty (score of 2), b) nerves analyzed partially (score of 1), and c) nerves not identified (score of 0).

RESULTS
In all three nerves, the best sequence for the visualization of the cisternal and intraforaminal course was b-FFE, with 58%, 73%, 62%, and all together 64.3% success in showing the fascicles of the 9th–11th nerves. This sequence with a very short time of repetition, symmetrical and balanced gradient around the echo time allowed very fast imaging and a high signal to noise ratio. T2W TSE sequence was superior to the DRIVE T2W sequence in assessing the cisternal and intraforaminal part of all three nerves. Post-contrast T1W sequence was probably the worst sequence in showing all three nerves.

CONCLUSION
b-FFE gradient echo MRI sequence with high spatial resolution is the optimal sequence for determining the courses of 9th–11th cranial nerves.

Key words: • *magnetic resonance imaging* • *cranial nerves* • *skull base*

From the Radiology Clinic (S.S. ✉ *sipahioglu_serdar@yahoo.com*), Dışkapı Yıldırım Beyazıt Training and Research Hospital, Ankara, Turkey.

Received 25 March 2009; revision requested 30 June 2009; revision received 27 October 2009; accepted 31 October 2009.

Published online 26 July 2010
DOI 10.4261/1305-3825.DIR.2744-09.3

The ninth, tenth and eleventh nerves have much in common functionally and share a nucleus that originates in the medulla. They are therefore considered as a group and are evaluated as a region. Together, they enter the jugular foramen (1, 2). Detecting the individual cranial nerves in the intraforaminal portion of the jugular foramen is useful in diagnostic imaging; however, visualization using conventional magnetic resonance imaging (MRI) protocols does not provide adequate details of the individual nerves (3, 4). With the rapid development of MRI technology, newer 2D-3D, high spatial resolution, strong T2-weighted (T2W) sequences have been developed; these include 3D-CISS (three-dimensional constructive interference in steady state), 3D-MP-RAGE (three-dimensional magnetization-prepared rapid gradient-echo) and 3D-FIESTA (three-dimensional fast imaging employing steady-state acquisition) (3–7). Both balanced fast-field echo (bFFE) and 3D-T2W-driven equilibrium radiofrequency reset pulse (DRIVE) sequences can also provide heavily T2-weighted, good MR cisternographic images and can be used to evaluate cranial nerve nuclei and root entry zones (6–8).

In this study, we aimed to assess the most efficient sequence for evaluating and visualizing the ninth, tenth and eleventh nerves. For this purpose, we evaluated images of this area on both sides of 100 patients. We applied bFFE, 3D-T2W-DRIVE, 2D-T2W-TSE and post-contrast T1-weighted (T1W) sequences and chose the best sequence for precisely visualizing all three nerves.

Materials and methods

Six hundred cranial nerves (9th, 10th and 11th) on both sides of 100 patients with complaints of tinnitus and hearing loss but without neurovascular compression syndromes were included in this study. All patients were referred to us with temporal MRI session requests by physicians. A total of 47 males and 53 females were analyzed between July and December 2008. The age range of the subjects was 14 to 74 years, and the mean age was 50 years. Informed consent was obtained prior to the MRI sessions. All MRI sections were performed using a 1.5-T Philips Nova Dual HP MRI scanner (16-channel Achiva Master, Eindhoven, Netherlands) with a 33 mT/m maximum gradient strength and a 180 mT/m per millisecond slew rate, using a standard head coil. We obtained MR images with bFFE, 3D- T2W DRIVE, 2D-T2W TSE and post-contrast T1W sequences. For the post-contrast series, 0.1 to 0.2 mmol/kg gadolinium-DTPA (Magnevist®, Schering-Bayer, Leverkusen, Germany; and Omniscan™, GE Healthcare, Waukesha, Wisconsin, USA)) was administered.

The parameters for the bFFE sequence were as follows: TR/TE/averages, 7.1/3.5 ms/3; flip angle, 50°; matrix, 308x320; field of view, 18x25 cm; reconstruction field of view, 83%; number of signals averaged (NSA,

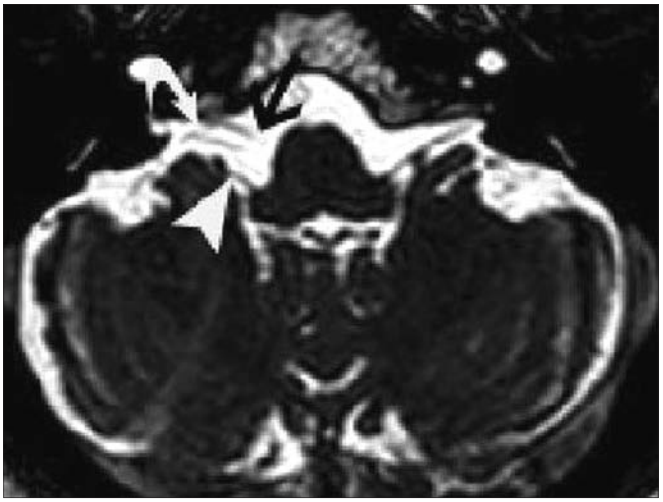

Figure 1. bFFE MRI sequence. The ninth *(black arrow),* tenth *(curved white arrow)* and eleventh *(white arrowhead)* nerves can easily be seen.

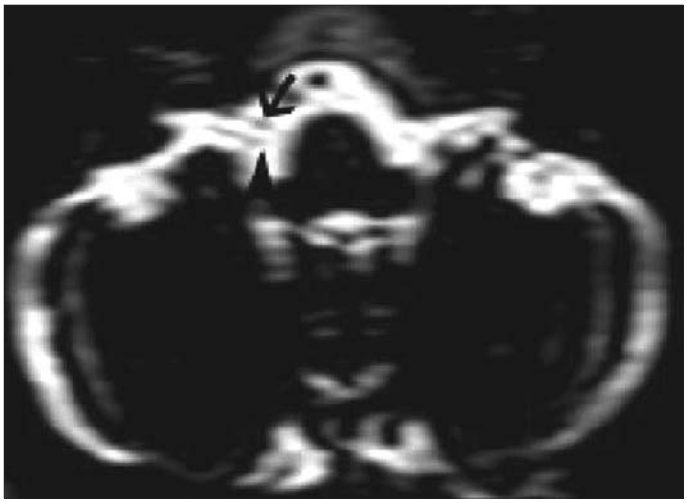

Figure 2. T2-weighted DRIVE MRI sequence shows the ninth *(arrow)* and tenth *(arrowhead)* nerves.

NEX), 3; slice thickness, 1.0 mm; number of partitions, 40. The scan time was 1.03 min.

The parameters for the 3D-T2W DRIVE sequence were as follows: TR/TE, 1500/250 ms; field of view, 13x13 cm; reconstruction field of view, 100%; NSA, 2; matrix, 256x256; slice thickness, 1.4 mm; turbo spin echo factor, 74; flip angle, 90°; number of partitions, 30. The scan time was 1.23 min.

The parameters for the 2D-T2W TSE sequence were as follows: TR/TE, 3000/120 ms; field of view, 14.8x17.5 cm; reconstruction field of view, 124%; NSA, 6; matrix, 168x256; slice thickness, 2.0 mm; turbo spin echo factor, 17; flip angle, 90°; number of partitions, 12. The scan time was 1.24 min.

The parameters for the post-contrast T1W FSE sequence were as follows: TR/TE, 450/30 ms; field of view, 14.8x10.5 cm; reconstruction field of view, 123%; NSA, 6; matrix, 128x256; slice thickness, 2.0 mm; turbo spin echo factor, 3; flip angle, 90°; number of partitions, 12. The scan time was 1.44 min.

Statistical analysis was performed applying the chi-square test, using SPSS version 11.5 (SPSS, Inc., Chicago, USA). $P < 0.01$ was considered a statistically significant difference.

Image analysis

The analysis of the data set obtained with all sequences was based on original axial images with an effective thickness between 1.0 and 2.0 mm. bFFE and T2W-DRIVE sequences are based on 3D images; post-contrast T1W and T2-FSE sequences are based upon 2D images. Because the duration of scans takes longer when 3D sequences are used, about five times longer for the post-contrast series and three times longer for the T2W-FSE series, we preferred to use 2D pulses instead of 3D sequences in the post-contrast T1W and T2W-FSE sequences in our study.

Three evaluation criteria were used in determining the intraforaminal courses of the ninth–eleventh cranial nerves. The criteria were as follows: a) localization of the nerves: the ninth cranial nerve is believed to be the most anteriorly positioned nerve, the tenth nerve is at the mid-line and the eleventh cranial nerve is expected to be at the postero-inferior side of the jugular foramen; b) demarcation of the nerves: related to the exact delineation, views range from distinct to unrecognizable in the displaying of nerve fascicles; and c) contrast with surrounding nerve structures: the root exit zone and the complete courses of the nerves through the cerebrospinal fluid (CSF) and their differentiation from the surroundings were denoted. The visualization of the ninth to the eleventh cranial nerves in their intrajugular foraminal courses was independently evaluated by two radiologists from MRI sequences generated by bFFE, 3D-T2W DRIVE, 2D-T2W TSE and post-contrast T1W. When disagreements occurred, a third neuroradiologist made the final evaluation. Each evaluation was graded and scored as follows: nerves identified with certainty (score of 2, nerves completely visualized in both sides), some of the nerves probably identified (score of 1, nerves partially visualized in both sides or exactly visualized in only one side) and nerves could not be identified on either side (score of 0).

The variance analysis test between dependent groups was performed for the results of both evaluators, and both evaluators gave quite similar scores.

Results

When visualizing the ninth (glossopharyngeal) nerve, we identified 116 nerves in 58 patients with a score of 2 (58%, Fig. 1) and 64 nerves with a score of 1 (32%) using the b-FFE sequence. Twenty nerves from 10 patients were not identified (score of 0) with this sequence. With the T2W-DRIVE TSE sequence, 98 nerves from 49 patients received a score of 2 (49%, Fig. 2), and 72 nerves from 36 patients received a score of 1 (36%); 30 glossopharyngeal nerves were not identified (score of 0). Using the T2W TSE sequence, glossopharyngeal nerves were clearly identified with a score of 2 in 98 cases (49%, Fig. 3), while 92 nerves were identified with a score of 1 (46%); the nerves were not identified in only 5 patients (score of 0, 5%). Using post-contrast T1W sequences, 34 nerves from 17 patients were clearly identified with a score of 2 (17%, Fig. 4), 130 nerves were identified with a score of 1 (65%) and 36 nerves were not identified in 18 patients (score of 0, 18%). These data are presented in Table 1 and Fig. 5a.

For the tenth cranial nerve, we clearly identified 146 vagus nerves with a score of 2 (73%) and 46 nerves with a score of 1 (23%); 8 nerves from 4 pa-

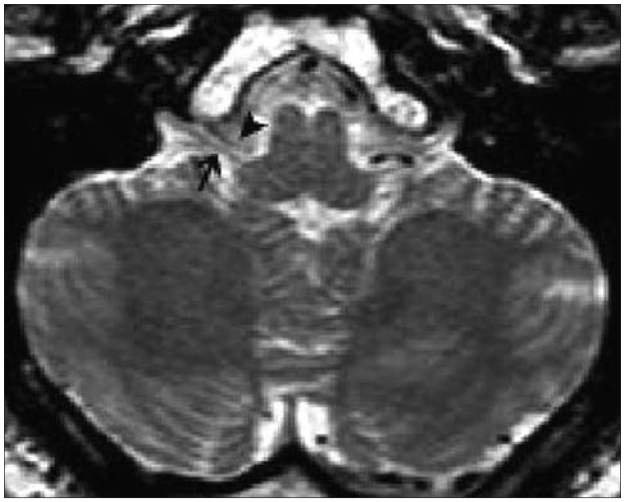

Figure 3. T2-weighted TSE MRI sequence shows the ninth *(arrowhead)* and tenth *(arrow)* nerves.

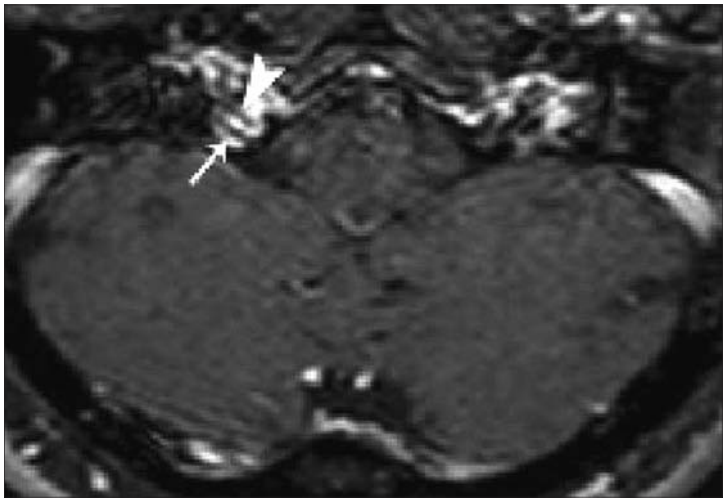

Figure 4. Post-contrast T1-weighted MRI sequence shows the right tenth *(arrowhead)* and eleventh *(arrow)* nerves.

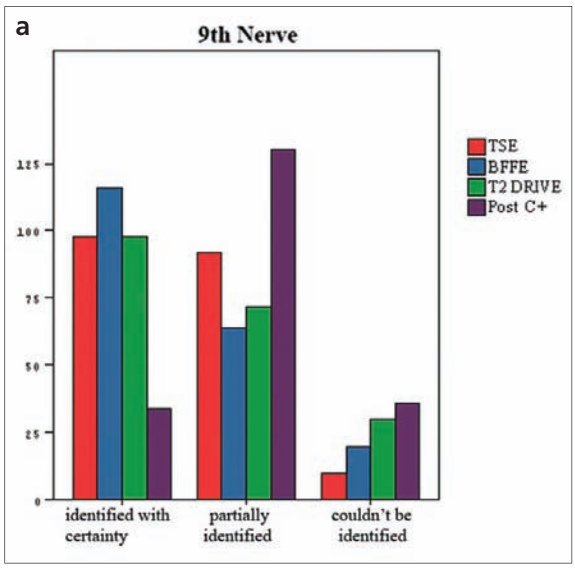

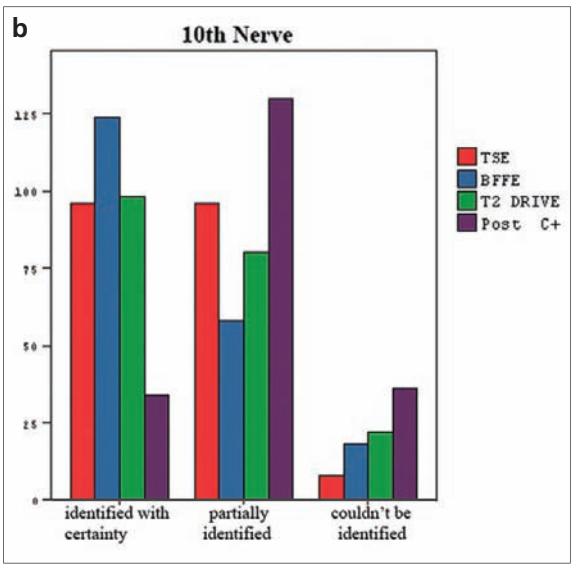

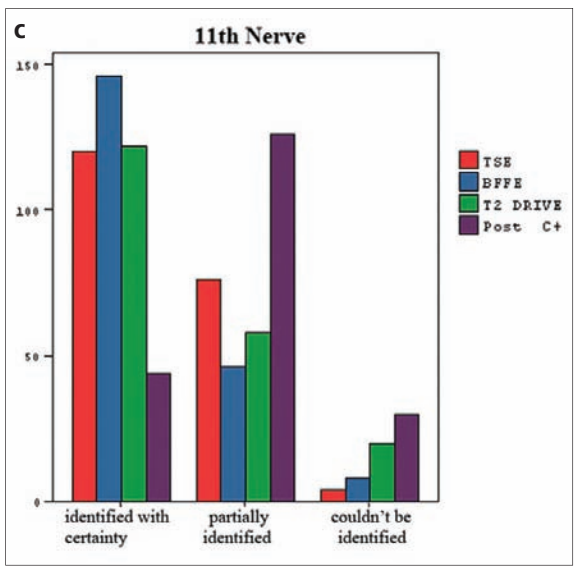

Figure 5. a–c. Success rate of visualization of the ninth **(a)**, tenth **(b)** and eleventh **(c)** nerves using different MRI sequences.

Table 1. The total number of nerves according to their visualization status

		Nerves		
		9th	10th	11th
Identified with certainty	TSE	98	92	10
	bFFE	116	64	20
	DRIVE	98	72	30
	Post-contrast	34	130	36
Partially identified	TSE	120	76	4
	bFFE	146	46	8
	DRIVE	122	58	20
	Post-contrast	44	126	30
Could not be identified	TSE	96	96	8
	bFFE	124	58	18
	DRIVE	122	80	22
	Post-contrast	44	130	36

tients were not identified (score of 0) using the b-FFE sequence. With the T2W-DRIVE TSE sequence, 122 nerves from 61 patients were identified with a score of 2 (61%), and 58 nerves were identified with a score of 1 (29%); 20 vagus nerves were not identified in 10 patients (score of 0). Using the T2W TSE sequence, the vagus nerve was clearly identified in 120 cases (score of 2, 60%), 76 nerves were identified with a score of 1 (38%) and only 4 nerves from 2 patients were not identified (score of 0). With the post-contrast T1W sequences, 44 nerves from 22 patients were clearly identified with a score of 2 (22%), 126 nerves were identified with a score of 1 (63%), and 30 vagus nerves were not identified (score of 0, Table 1, Fig. 5b).

In the case of the eleventh nerve, we identified 124 nerves with a score of 2 (62%) and 58 nerves with a score of 1 (29%) using the bFFE sequence; 18 accessory nerves were not identified (score of 0). With the T2W-DRIVE TSE sequence, 98 nerves from 49 patients were identified with a score of 2 (49%), 80 nerves from 40 patients were identified with a score of 1 (40%), and 22 accessory nerves were not identified (score of 0). Using the T2W TSE sequence, the accessory nerve was clearly identified with a score of 2 in 96 cases (48%); 96 bilateral nerves were identified with a score of 1 (48%), and only 8 nerves were not identified (score of 0). Using the post-contrast T1W sequences, 34 nerves were clearly identified (score of 2, 17%), 130 nerves were identified with a score of 1 (65%), and 36 accessory nerves were not identified (score of 0). These results are shown in Table 1 and Fig. 5c.

The chi-square test proved to be effective for determining the statistical differences between the results obtained using different imaging modalities to analyze the ninth, tenth and eleventh cranial nerves because the number of chi-square test cells with frequency lower than 5 was less than 20% of all cells in all groups. With statistically significant difference set at the 0.01 level, there are significant differences in the effectiveness of the imaging procedures used to visualize the three cranial nerves. At this level, the most effective sequence for visualizing all three nerves is the bFFE (Table 2, Fig. 5).

Table 2. Statistical analysis of nerve visualization using different imaging sequences

				MRI sequence						
Nerves				TSE	bFFE	DRIVE	Post-contrast	Total	SD	*P*
9th	Observation	Identified with certainity	n	98	116	98	34	346	6	0.000
			%	28.3%	33.5%	28.3%	9.8%	100.0%		
		Partially identified	n	92	64	72	130	358		
			%	25.7%	17.9%	20.1%	36.3%	100.0%		
		Could not be identified	n	10	20	30	36	96		
			%	10.4%	20.8%	31.3%	37.5%	100.0%		
	Total		n	200	200	200	200	800		
			%	25.0%	25.0%	25.0%	25.0%	100.0%		
10th	Observation	Identified with certainity	n	120	146	122	44	432	6	0.000
			%	27.8%	33.8%	28.2%	10.2%	100.0%		
		Partially identified	n	76	46	58	126	306		
			%	24.8%	15.0%	19.0%	41.2%	100.0%		
		Could not be identified	n	4	8	20	30	62		
			%	6.5%	12.9%	32.3%	48.4%	100.0%		
	Total		n	200	200	200	200	800		
			%	25.0%	25.0%	25.0%	25.0%	100.0%		
11th	Observation	Identified with certainity	n	96	124	98	34	352	6	0.000
			%	27.3%	35.2%	27.8%	9.7%	100.0%		
		Partially identified	n	96	58	80	130	364		
			%	26.4%	15.9%	22.0%	35.7%	100.0%		
		Could not be identified	n	8	18	22	36	84		
			%	9.5%	21.4%	26.2%	42.9%	100.0%		
	Total		n	200	200	200	200	800		
			%	25.0%	25.0%	25.0%	25.0%	100.0%		

SD, standard deviation

The results of the 2D-T2W TSE and T2W-DRIVE sequences are quite similar; therefore, to choose the second most effective sequence for clearly identifying nerves, we added the 'partially identified' results (score of 1) to the 'clearly identified' results (score of 2). By so doing, we determined that T2W TSE sequence is the second most effective sequence and is superior to the T2W-DRIVE sequence ($P < 0.01$). The post-contrast T1W sequence is probably the least effective sequence for identifying all three nerves ($P < 0.01$).

Discussion

Because of its high spatial resolution and contrast advantages, MRI is the gold standard for visualizing the cisternal and intraforaminal parts of the glossopharyngeal, vagus and accessory nerves. Newer MRI sequences and MR cisternography can easily show the anatomic and pathologic relationships of the neural roots to the adjacent vessels, duramater and the courses of all nerves in the jugular foramen (6, 9, 10).

For routinely depicting the ninth, tenth and eleventh cranial nerves, heavily T2W sequences may be important because of their high sensitivity in detecting the cranial nerve nuclei and root entry zones and their foraminal courses (5–7, 9–11).

Using high spatial resolution and heavily T2W sequences, the trunks of all three nerves and their courses in the jugular foramen can be detected quite accurately (6, 9, 10).

Currently, sequences with steady state free precession (SSFP) and the DRIVE techniques are generally preferred (5–7, 9). SSFP sequences are basically gradient echo sequences, and bFFE, BTFE, True FISP, FIESTA are the most frequently commercially used sequences (5–10). Using a large flip angle, very short time of repetition (TR) and a symmetrical and balanced gradient around the echo time (TE), an SSFP regime can be achieved that allows very fast imaging. A high signal-to-noise ratio (SNR) can be obtained (5–7, 10). This type of imaging provides very high signals from tissues with large T2/T1 ratios, such as fluid, blood and fat. Therefore, SSFP imaging can be used to visualize the cisternal segments of cranial nerves because of its excellent CSF-nerve contrast and high spatial resolution (6, 7, 9, 10). Scanning time is quite short, and cisternal segments of the cranial nerves are depicted clearly (5–7, 10). In our study, bFFE sequence with 1-mm slice thickness and very short TR-TE supplied very good contrast between the jugular nerve complex and the surrounding CSF and showed the highest spatial resolution of the sequences used in this study.

When DRIVE is applied at the end of a TSE echo train, it accelerates the relaxation and returns the magnetization to equilibrium (8). DRIVE is based on a 3D TSE sequence applying a set of recovery pulses that push the residual transverse magnetization back to the longitudinal axis (6, 8). DRIVE makes a T2 contrast to TSE sequences, and CSF is brighter (6).

The basic principle of cranial nerve visualization is to obtain heavily T2W images with high CSF signal and few artifacts. The shortened TR reduces flow void artifacts, further increasing the brightness of fluids; it also decreases the scan time while preserving high fluid signal, making less time available for flow voids caused by CSF motion and recovery of magnetization at the end of a long echo train (6, 8). In our study, the 3D-T2W DRIVE sequence with 1.4-mm slice thickness, higher TSE factor and smaller field of view (FOV) supplied the highest spatial resolution, but it was less successful at detecting the jugular nerve complexes than were the bFFE and T2W TSE sequences.

2D-T2W FSE sequences provide relatively low spatial resolution and have the disadvantages of losing signals emanating from fluids (mainly due to flow voids), saturation and magnetization transfer effects. 3D-TSE sequences overcome these obstacles, but the scans take longer (8, 9). Because the 2D-T2W TSE sequence required less time, we utilized it in this study. We attempted to increase the spatial resolution by using 2-mm slice thickness, more excitations and relatively lower FOV. With these modifications, we found that 2D-T2W TSE was the second-best sequence for identifying the jugular foramen nerve complexes.

The post-contrast T1W-FSE sequence provides the lowest spatial resolution because the CSF, blood and the surrounding tissues appear darker due to their higher transverse relaxation and their longer T1 times; therefore, we could not generate good CSF-nerve contrast using this technique (3, 6). We tried to increase the spatial resolution in this sequence by using low TE, 2-mm slice thickness, more excitations and small FOV; nevertheless, we found that, of the sequences we tested, this sequence was the poorest for identifying the jugular nerve complexes. Post-contrast T1W sequences are, however, very useful for detecting masses in the jugular foramen and jugular bulb because the mass lesions in the foramen and bulb are strongly enhanced. Post-contrast T1W sequences also provide important information in cases of nerve impairment, inflammation, vessel compression, cerebral pathologies such as infarction or demyelinating lesions, and perineural spread of head and neck malignancies (9–12).

Few reports have been published concerning MRI of the glossopharyngeal-vagus and accessory nerves. Yousry et al. (9) identified the ninth, tenth and eleventh cranial nerves as the 'lower nerve complex' and visualized this complex 100% using the 3D-CISS sequence and 52.5% (21 of 40) using T2W FSE sequences; with the T2W FSE sequence, eight lower complex nerves were partially visualized (20%, 8 of 40). These authors' visualization rates for the lower nerve complex using the 3D-CISS sequence are more successful than ours for all sequences; however, their T2W FSE results are less successful than our findings for the ninth, tenth and eleventh nerves using the 2D-TSE sequence.

Studying 25 volunteers, Cheng et al. (10) were completely successful in identifying the jugular nerve complexes using the 3D-FIESTA sequence; 12% of the nerve complexes were probably identified, and 88% were clearly identified. With 2D-FSE sequence, this study identified 85% of the nerve complexes; 47% of the nerve complexes were probably identified, and 38% were clearly identified. Like those of Yousry et al., these authors' 3D-FİESTA results for visualizing the nerve complex are superior to our sequence results, but our findings in visualizing the nerve complex with the 2D-T2W TSE sequence are far superior (9, 10).

In their 50-patient study, Hatipoglu et al. (6) used the 3D-FIESTA sequence and succeeded in visualizing 100% of the lower nerve complexes; 96% were completely identified, and 4% were partially identified. With T2W FSE, this study reported a 67% success rate (55%

total, 12% partially identified). As in the studies described above, these 3D-FIESTA results yielded a higher visualization rate than our bFFE and 3D-T2W DRIVE findings; however, the incidental findings with T2W FSE reported in this study are inferior to our 2D-T2W TSE results.

Davagnanam and Chavda (3) studied the ninth to the eleventh cranial nerves of ten patients undergoing routine follow-up imaging for vestibular schwannomas using contrast-enhanced 3D-FIESTA sequences and showed the nerve complex in all cases. He thought that the 3D-FIESTA sequence was much more effective after contrast application and that it may be the sequence of choice in identifying the lower cranial nerves. In our opinion, however, assessment with only ten patients cannot show the sensitivity and specificity of this sequence.

Fischbach et al. (13) studied a total of 16 glossopharyngeus-vagus complexes of 12 healthy volunteers using 1.5-T and 3.0-T MRI systems. These authors used both T2W FSE and fast recovery-fast spin echo (FRFSE) sequences. With the 1.5-T system, they were 80% successful in FSE and 100% successful in FRFSE sequences. With the 3.0-T system, the success rate increased to 90% with FSE and remained at 100% for FRFSE. They determined that the 3.0-T system is more accurate and that the FRFSE sequence is better for visualizing nerves. Their results with both the 1.5- and 3.0-T systems are superior to our T2W TSE and T2W DRIVE sequences.

The FRFSE sequence (fast-recovered fast spin-echo) is a modified FSE sequence from GE Healthcare and is used here for T2W imaging (13). In this sequence, once the final echo had been acquired, an additional 180° radiofrequency (RF) pulse refocuses the residual magnetization in the transverse plane; a 90° RF pulse then flips the proton back to the longitudinal axis rather than allowing it to undergo T1W recovery. It reduces the transverse magnetization in the longitudinal axis, thus accelerating the longitudinal magnetization. This sequence results in good contrast with short scan time and shorter TE (13, 14). Similar pulse sequences are 'RESTORE' in Siemens and 'DRIVE' in Philips Medical Systems.

Gradient echo imaging techniques such as bFFE in 3.0-T systems have some major problems. Gradient echoes have a lower SAR (specific absorption rate), stronger susceptibility effects and more artifacts, including a larger chemical shift. In addition, they are more sensitive to field inhomogeneities and have a reduced crosstalk, so a small or no-slice gap can be used. As the flip angle is decreased, T1 weighting can be maintained by reducing the TR. T2*-weighting can be minimized by keeping the TE as short as possible, but pure T2-weighting is not possible (13, 15, 16). Other potential obstacles include a higher RF deposition-conductivity effect due to the shorter wavelengths, decreased speed of electromagnetic radiation, increased tissue T1 relaxation times and dielectric resonances (15, 16). In 3.0-T systems, the gain in SNR will be higher in T2W sequences than in T1W sequences because longer TRs allow more complete recovery of the longitudinal magnetization and transverse relaxation times (T2) are fairly independent of the main magnetic field strength (15). Three-dimensional gradient echo acquisition and a small FOV to reduce increased susceptibility effects should overcome the weaknesses of these 3.0-T system sequences (16).

To the best of our knowledge, our study is the first that attempts to determine the best sequence for visualizing the cisternal and intraforaminal courses of the lower nerve complex (9–11th nerves). We applied the following four sequences to 100 patients: bFFE, 3D-T2W DRIVE, 2D-T2W TSE and post-contrast T1W; we then attempted to analyze 600 bilateral nerves.

Our results show that the post-contrast T1W series was the least effective in visualizing the ninth, tenth and eleventh cranial nerves. Only 112 nerves were completely visualized with this series; these included 34 of the 9th, 44 of the 10th and 34 of the 11th cranial nerves. With the T2W DRIVE, we completely visualized 320 nerves, 98 of both the 9th and 11th nerves and 122 of the 10th nerves. With the 2D-T2W TSE sequence, we completely visualized 314 nerves: 98 of the 9th, 120 of the 10th and 96 of the 11th cranial nerves. With the T2W DRIVE sequence, we partially identified 210 nerves, and with the T2W 2D-TSE sequence, we partially identified 264 jugular nerve complexes. Using the bFFE sequence, we clearly depicted 386 nerves: 116 of the 9th nerves, 146 of the 10th nerves and 124 of the 11th nerves. With this sequence, we visualized the entire lower nerve complex in 64.3% of patients.

Use of the bFFE sequence has many advantages in determining the cisternal and intraforaminal courses of the ninth-eleventh nerve complexes compared to the other sequences. 2D-T2W TSE is superior to the T2W-DRIVE sequence in identifying the lower nerve complex of the ninth-eleventh cranial nerves.

In conclusion, bFFE, a SSFP gradient echo sequence of high spatial resolution and short scanning duration, is the sequence of choice in assessing the cisternal and intraforaminal parts of the ninth, tenth and eleventh nerves. In our study, we were successful in 58%, 73% and 62% of cases at visualizing the ninth, tenth and eleventh nerves, respectively. Compared to other sequences, bFFE sequence has many advantages for visualizing the ninth–eleventh cranial nerves. The T2W TSE sequence is the second choice and is superior to the T2W-DRIVE images. 3D- T2W DRIVE is far better at visualizing all the nerves than is the post-contrast T1W series. The worst sequence is the post-contrast T1W series; for assessing the ninth, tenth and eleventh nerves, contrast agent application has only limited value.

Acknowledgements

We are grateful to Mr. Haydar Polat and Mr. Egemen Alper for their assistance with the figures. We would also like to thank Ms. Melahat Unlu of Philips Medical Systems for technical support.

References

1. Laine FJ, Underhill T. Imaging of the lower cranial nerves. Magn Reson Imaging Clin N Am 2002; 10:433–449.
2. Laine FJ, Smoker WRK. Anatomy of the cranial nerves. Neuroimaging Clin N Am 1998; 8:69–100.
3. Davagnanam I, Chavda SV. Identification of the normal jugular foramen and lower cranial nerve anatomy: contrast-enhanced 3D fast imaging employing steady-state acquisition MR imaging. AJNR Am J Neuroradiol 2008; 29:574–576.
4. Seitz J, Held P, Fründ R, et al. Visualization of the IXth to XIIth cranial nerves using 3-dimensional constructive interference in steady state, 3-dimensional magnetization-prepared rapid gradient echo and T2-weighted 2-dimensional turbo spin echo magnetic resonance imaging sequences. J Neuroimaging 2001; 11:160–164.
5. Mikami T, Yoshihiro M, Yamaki T, et al. Cranial nerve assessment in posterior fossa tumours with fast imaging employing steady-state acquisition (FIESTA). Neurosurg Rev 2005; 28:261–266.

6. Hatipoglu HG, Durakoglugil T, Ciliz D, Yuksel E. Comparison of FSE T2W and FIESTA sequences in the evaluation of posterior fossa cranial nerves with MR cisternography. Diagn Interv Radiol 2007; 13:56–60.
7. Tsuchiya K, Aoki C, Hachiya J. Evaluation of MR cisternography of the cerebellopontine angle using a balanced fast-field-echo sequence: preliminary findings. Eur Radiol 2004; 14:239–242.
8. Ciftci E, Anik Y, Arslan A, et al. Driven equilibrium (DRIVE) MR imaging of the cranial nerves V-VIII: comparison with the T2-weighted 3D TSE sequence. Eur J Radiol 2004; 51:234–240.
9. Yousry I, Camelio S, Schmid UD, et al. Visualization of cranial nerves I-XII: value of 3D-CISS and T2-weighted FSE sequences. Eur Radiol 2000; 10:1061–1067.
10. Yu Shu C, Zheng-rong Z, Wei-jun P, Feng T. Three-dimensional fast imaging employing steady-state acquisition and T2-weighted fast-spin echo magnetic resonance sequences on visualization of cranial nerves III-XII. Chin Med J 2008; 121:276–279.
11. Harnsberger HR. The lower cranial nerves (VII–XII). In: Osborn AG, Bragg DG, eds. Handboooks in radiology: head and neck imaging. Chicago: Yearbook Medical Publishers, 1995; 488–521.
12. Remley KB, Latchaw RE. Imaging of the cranial nerves IX, X, XI. Functional anatomy and pathology. Neuroimaging Clin N Am 1993; 3:171–191.
13. Fischbach F, Muller M, Bruhn H. Magnetic resonance imaging of the cranial nerves in the posterior fossa: a comparative study of T2-weighted spin echo sequences at 1.5 T and 3.0 T. Acta Radiol 2008; 3:358–363.
14. Huang HI, Emery KH, Laor T, et al. Fast-recovery fast-spin echo T2 weighted MR imaging: a free-breathing alternative to fast-spin echo in the pediatric abdomen. Eur Radiol 2008; 38:675–679.
15. Merkle EM, Dale BM. Abdominal MRI at 3.0T: the basics revisited. AJR Am J Roentgenol 2006; 186:1524–1532.
16. Mountford EC, Stanwell P, Ramadan S. Breast MR imaging at 3.0T. Radiology 2008; 248:319–320.